Proceedings of ICRC 2001: 2618 © Copernicus Gesellschaft 2001

ICRC 2001

TeV γ and X-ray flaring of Mrk 421 April 2000

D. J. Fegan [1], **G. Fossati**[2], **and the VERITAS collaboration**[3]

[1]UCD, Belfield, Dublin 4, Ireland.
[2]UCSD, La Jolla, CA 92093-0424 USA.
[3]Whipple Observatory, Amado, AZ, 85645, USA

Abstract. Evidence for correlated TeV γ and X-ray flaring of the extreme blazar Mrk421 during April 2000 is presented and discussed. The remarkably persistent TeV flare of April 30th 2000 (40 σ significance), exhibiting structure over almost six hours of continuous observation, is analysed in detail.

1 Extreme BL Lac objects

The most extreme members of the Active Galactic Nucleus (AGN) family are BL Lac objects and optically violently variable (OVV) quasars, collectively known as blazars. These objects are dominated by the presence of relativistic jets. For jets fortuitously aligned with an observers line of sight, emission may exhibit dramatic variability over very short time scales, in turn implying remarkably compact emission regions. For blazars, the Spectral Energy Distribution (SED) is dominated by non-thermal continuum emission, extending from radio to TeV gamma rays. The broadband nature of the blazar emission offers unique insights into energetic physical processes at work in a very compact region, close to the base of the jet and near the underlying central engine, most likely a supermassive black hole. BL Lacs are very effectively characterized on the basis of their SED shape. X-ray and radio flux limited surveys apear to display a bimodal distribution of properties, with LBL (Low-energy peaked, or "Red" BL Lacs) having synchrotron peaks in the IR-optical bands, and HBL (High-energy peaked, or "Blue" BL Lacs) in the UV to soft X-ray band. Recent comprehensive surveys such as DXRBS, REX and RGB have extended, by almost two orders of magnitude, the range of observable synchrotron peak frequencies. For blazar class objects, broadband emission confirms that the synchrotron peak may span the entire IR X-ray range, thus accounting for the multi-frequency emission properties of this class of object. Mrk421, Mrk501, 1ES2344 and 1H1426 all exhibit broadband emission properties, high synchrotron peak frequencies and have been observed to flare at TeV energies and may therefore be classified as extreme objects.

Correspondence to: D. J.Fegan (djfegan@ferdia.ucd.ie)

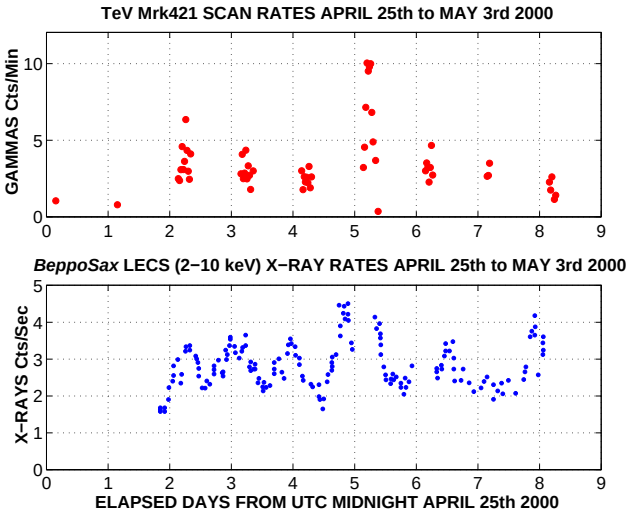

Fig. 1. Contemporaneous Mrk421 TeV γ and X-ray lightcurves.

2 TeV emission from extreme BL Lac objects

While high synchrotron peak frequencies characterise extreme BL Lac objects as potentially good candidates for TeV emission through the inverse Compton mechanism, source variability and flaring also play a predominant role. Among the most productive and exciting results in astrophysics have been multiwavelength observations of blazar activity, where a range of instrumentation has been utilised to simultaneously monitor targeted blazars. Multiwavelength campaigns underpin determination of source SEDs and searches for correlated multiwavelength variability. The importance of multiwavelength campaigns from the perspective of TeV astrophysics is well documented in Catanese and Weekes (1999), Buckley (1999) and Weekes (2000), particularly in relation

to Mrk421 and Mrk501. Evidence for correlated TeV and X-ray variability in Mrk421 has also been previously observed by Buckley et al., (1996), Maraschi et al., (1999), Catanese and Weekes (1999) and Krawczynski et al., (2001).

3 Mrk421 multiwavelength data, April 2000.

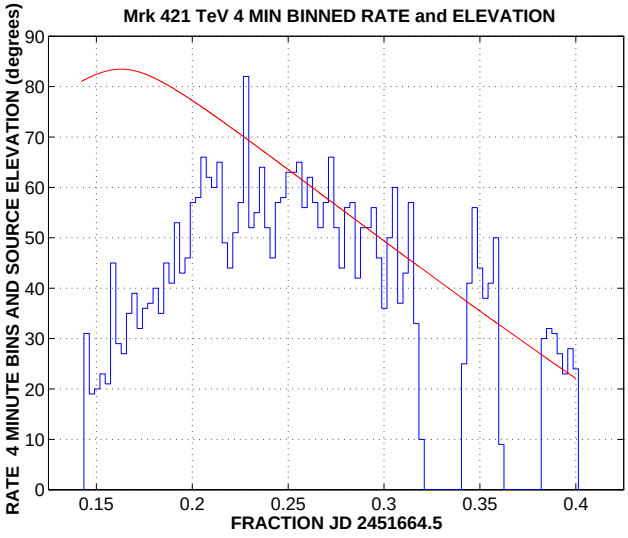

Fig. 2. Mrk TeV γ lightcurve April 30th 2000.

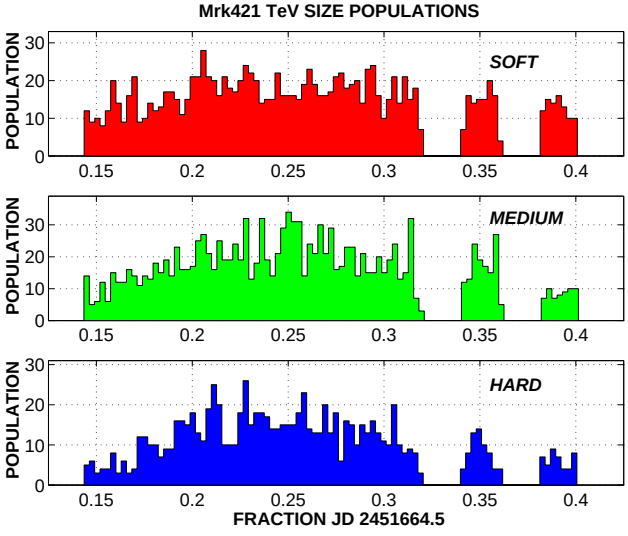

Fig. 3. Mrk421 TeV γ-ray Log10(size) bands April 30th 2000. SOFT - ≤ 2.75; MEDIUM between 2.75 and 3.00; HARD ≥ 3.0

3.1 TeV γ-ray data.

Observations of Mrk421 are routinely made using the 10 m Imaging Atmospheric Cerenkov Telescope (IACT) at the Whipple Observatory (Cawley et al., 1990). The current GRANITE III camera configuration is a 490 pixel instrument with an inner field of view of 2.6° (379 13 mm PMTs) and an outer region (111 28 mm PMTs) resulting in a total field of view of 4.0° (Finley et al., 2001). Data is acquired in two possible observational modes, ON/OFF or TRACKING. In the former mode, a source is observed for 28 minutes (ON) followed two minutes later by observing a reference region of sky (OFF), also for 28 minutes. Subtracting OFF data from ON data facilitates detection of excess events from a source. In tracking mode the source is continuously observed and data recorded as 28 minute scans. Tracking observations are predominantly made when a source is unusually active.

γ-ray ray events are isolated from the dominant hadronic isotropic background following image cleaning and parameterisation (Fegan, 1997). The particular image parameterisation for the analysis described here is Supercuts2000, optimised for the 490 pixel camera (Catanese and Lessard, 2000). Events are selected on the basis of image shape and orientation. For showers detected out to zenith angles of 45° the most probable detected γ-ray energy is 430 GeV but some sensitivity persists down to energies as low as 100 GeV. Between April 25th to May 3rd 2000, a significant increase in TeV emission was observed from Mrk 421 (Fegan, 2000), with a spectacularly persistent flare being detected on April 30th. Attributes of this TeV transient form the main focus of this paper.

3.2 X-ray data.

BeppoSAX, the joint Italian-Dutch scientific X-ray satellite has been extensively described elsewhere (Boella et al., 1997). The principal coaligned instruments dedicated to X-ray detection are: (a) the Low Energy Concentrator Spectrometer (LECS, 0.1-10 KeV). (b) the Medium Energy Concentrator Spectrometer (MECS, 2-10 KeV) and (c) the Phoswich Detector System (PDS, 12 300 KeV).

Light curves are accumulated for each instrument with conventional choices of extraction radius and background subtraction (Fosatti et al., 2000). The BeppoSAX X-ray light curve for the period April 25th to May 3nd 2000 is used here for comparison with the TeV flare data. The data in question is from the LECS instrument, with energy sensitivity in the 2 - 10 keV range. Unfortunately, due to instrumential difficulties, it was not possible to acquire MECS data from that detector on April 30th. There are also two short dropouts in the LECS data records during both April 30th and May 1st (Fig.1). These do not seriously detract from the overall interpretation of the X-ray data.

4 The persistent flare of April 30th 2000

4.1 γ-ray and X-ray lightcurve correlation

Time correlation between γ-ray and X-ray lightcurves is evident from Fig.1. There is an underlying pattern of X-ray enhancement appearing to preceed the TeV enhancement over the observational interval in question. Quantifying the degree of correlation between lightcurves is difficult however, given the significant undersampling of the TeV lightcurve and the LECS data dropout. Nevertheless the close overlap in

time of the γ-ray transient and the X-ray emission profile on April 30th makes this region worthy of more detailed examination, on a finer resolution timescale. Most unfortunately, the first LECS data dropout coincides exactly with the TeV γ-ray flare observations. Turning on several hours before the TeV flare, the X-ray emission is boosted appreciably above levels detected on neighbouring days. Following the dropout, the decay of the X-ray emission occurs after the γ-ray flare observations ceased for the day.

4.2 The TeV lightcurve

The TeV observations of April 30th are unusual in that the rate increase is dramatic, rising from a quiescent average of less than 2.0 γ-rays per minute over a 28 minute scan to an average in excess of 10 γ-rays per minute at the peak of the flare. The TeV lightcurve for that day is displayed in Fig.2, in 4 minute bins. The full flare is composed of 3555 events spanning an interval of more than 22,280 seconds. Most of the data is made up of contiguous TRACKING scans, the two gaps in the data near the end of the observations corresponding to OFF scans. The flare exhibits a reasonably uniform rise to peak with a characteristic doubling time of about 1 hour. Superimposed on the rate histogram is the source elevation which reflects the source passing through culmination, thereafter setting, reaching a limiting elevation of 22° when observations ceased. This extremely low elevation has consequences which will be discussed later.

4.3 γ-ray event size distribution

For on-axis γ-rays there is a strong correlation between primary energy and total light intercepted by the imaging camera. The size of each detected event is estimated by summing the light in the inner 379 PMTs, and for shower images not severely truncated by edge effects, the size parameter is proportional to energy of the primary particle. Supercuts2000 applies an upper distance parameter cut in order to reject truncated images. γ-ray events may be sorted into three arbitrary size bins, labelled soft, medium and hard, on the basis of Log10(Size) values as follows : (a) $\leq$ 2.75, (b) between 2.75 and 3.0, and (c) $\geq$ 3.0. Fig.3 shows how events in each size band are distributed in time. At the beginning of observations the flare is more firmly established for the soft sample of photons than for the others. The medium sample exhibit a somewhat steeper growth rate to a broad maximum, the hard sample an even steeper growth rate. It is interesting for each size band population, to cumulatively sum events in each time bin across the full duration of the observation. Time dependent ratios may be formed of soft/medium, hard/medium and hard/soft running ratios - Fig.4. Naturally as the magnitudes of the cumulative sums grow, ratios become less prone to the influence of rate fluctuations and underlying trends should be discernable. The dominance of smaller sized events is seen to diminish with time relative to that of the larger sized population. For the first 2.5 hours of the flare the character of the data is evolving appreciably, the ratio of soft/hard

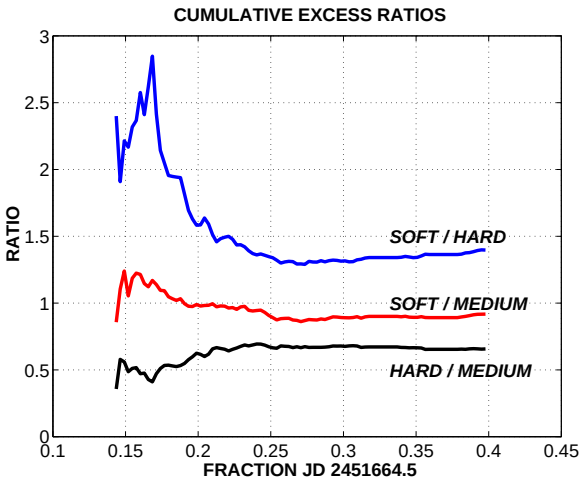

Fig. 4. Mrk421 TeV γ-ray event size band ratios.

decreasing dramatically. Normalised to the medium sized events, the influence of the soft component is decreasing while that of the hard component is increasing, over the same timescale. The source is above 60° for all this interval. For the final 3.5 hours of the flare the ratios are quite flat as the flare decays. Interpretation of behavior during the final 2 hours is complicated by the low elevation of the source.

5 The implications of Large Zenith Angle [LZA] observations

The Whipple collaboration have previously exploited the LZA technique in the detection of significant emission from Mrk421 at energies in excess of 5 TeV (Krennrich et al., 1997). Observations of Mrk421 on April 30th 2000 finished with three ON/OFF pairs taken in LZA mode, all having elevations below 40°. All selected events used to construct Figures 2, 3 and 4 were isolated using fixed parameter boundary cuts - Supercuts2000. However, the average shower energy increases significantly for LZA observations by comparison with SZA observations. Showers viewed at LZA develop higher in the atmosphere and are further away than those observed at SZA. The lateral extent of the image at maximum of development appears somewhat demagnified. Since the image shape parameters Length and Width are critical in any background rejection strategy, ideally they should be scaled to reflect the elevation. Diminution of the Length parameter is somewhat compensated for by a slight shift to larger impact parameters of showers at LZA, resulting in somewhat more elongated images, the further away the shower core is from the telescope. Both the energy threshold and the effective collection area of the telescope also increase at LZA.

The response of the GRANITE III camera at LZA has recently been modelled (Petry et al., 2001) by investigating the performance of the standard analysis at different elevation angles, using both simulations and real off-source data. In particular, improved background rejection has been accom-

plished by scaling some of the image parameter cuts (Length and Width) as a function of zenith angle of observation of the source, see Fig.6 in (Petry et al., 2001). Applied to the flare of April 30th 2000, the scaled imaging cuts result in a more effective rejection of background events at low elevation (Fig.5). Less events are passing the scaled image cuts by comparison with the unscaled. However, the detection statistical significance of each of the final ON/OFF pairs is still appreciable, 8.5, 7.5 and 3.5 σ respectively. At higher elevations, scaled cuts perform very similarly to unscaled. Fig.6 shows the scaled cut events histogrammed by event size, reflecting a reduction in detected numbers of events for all three size bands. However, ratios remain very similar to those shown in Fig.3 for unscaled cut data.

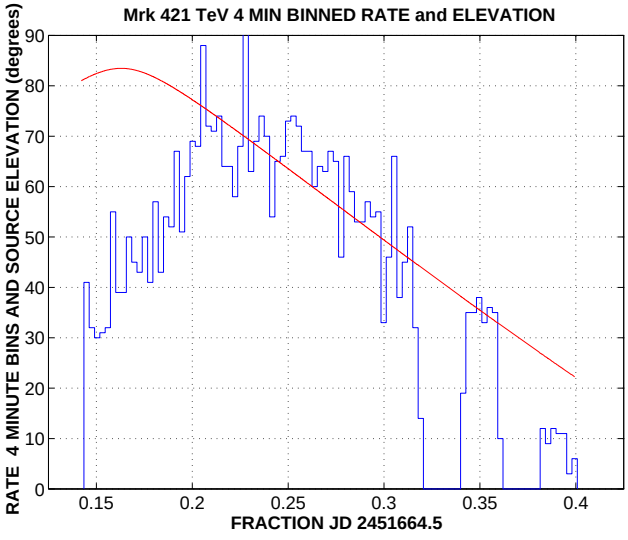

Fig. 5. Mrk TeV γ-ray lightcurve, scaled cuts.

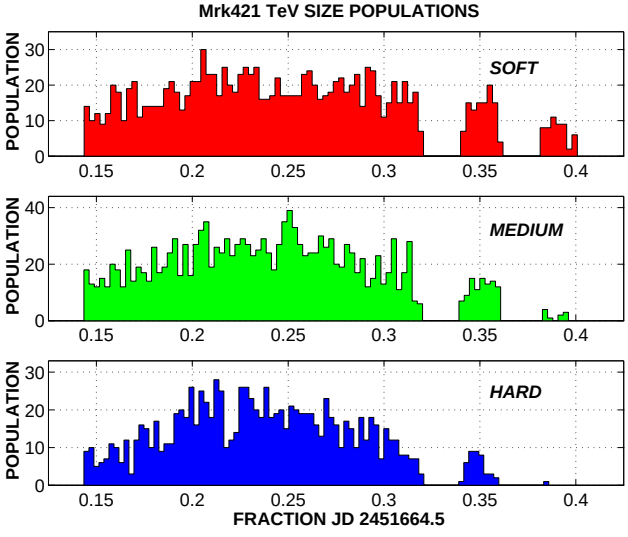

Fig. 6. Mrk421 TeV γ-ray size bands, scaled cuts.

6 Conclusions

Overlapping Whipple TeV γ and BeppoSax X-ray observations of Mrk421 during April 2000 show correlation and evidence for a major TeV flare on April 30th. The behavior is similar to flaring observed in 1994 by the Whipple collaboration (Kerrick et al., 1995) and to a pair of spectacular flares observed in May 1996 (Gaidos et al., 1996). The April 30th 2000 flare is remarkable in its persistence, lasting over 6 hours before observations terminated. The rise time is of the order of 2 hours, the decay time of the order of 3 hours with about one hour of plateau between. A subsequent TeV flare was observed by the Whipple collaboration on March 19th 2001 (Holder et al., 2001).

Acknowledgements. The VERITAS collaboration is supported by the U.S. Dept. of Energy, N.S.F., the Smithsonian Institution, P.P.A.R.C.(U.K.) and Enterprise-Ireland.

References

Boella, G., et al., A &AS, 122, 299, 1997.
Buckley, J.H., et al., ApJ, 472, L9, 1996.
Buckley, J.H. 26th ICRC AIP Conf. Proc. 516, 195, 1999.
Catanese, M. and Weekes, T.C. ASP 111, 1193, 1999.
Catanese,M. and Lessard,R. Private Communication 2000.
Cawley, M.F., et al., Exp. Ast, 1, 185, 1990.
Fegan, D.J. J.Phys.G. Nucl. Part. Phys. 23, 1013, 1997.
Fegan, D.J. IAU Telegram April 2000.
Finley, J.P., et al., Proc 27th ICRC (Hamburg) 2001.
Fosatti,G., et al., ApJ, 541, 153, 2000.
Gaidos, J.A. et al. Nature, 383, 319, 1996.
Holder, J. et al., Proc 27th ICRC (Hamburg) 2001.
Kerrick, A.D. et al. ApJ, 438, L59, 1995.
Krawczynski, H. et al., astro-ph/0105331 May 2001.
Krennrich,F. et al., ApJ, 481, 758, 1997.
Maraschi, L., et al., ApJ, 526, L81, 1999.
Petry, D. et al., Proc 27th ICRC (Hamburg) 2001.
Weekes, T.C. AIP Conf. Proc. 558, 15, 2001.